Fusion Engineering and Design 49–50 (2000) 689–695

Fusion Engineering and Design

www.elsevier.com/locate/fusengdes

ARIES-ST breeding blanket design and analysis

ARIES Team, M.S. Tillack [a,*], X.R. Wang [a], J. Pulsifer [a], S. Malang [b], D.K. Sze [c]

[a] *University of California, La Jolla, San Diego, CA 92093-0417, USA*
[b] *Forschungszentrum Karlsruhe, Postfach 3640, D-76021 Karlsruhe, Germany*
[c] *Argonne National Laboratory, 9700 S. Cass Ave., Argonne, IL 60439, USA*

Abstract

ARIES-ST is a 1000 MW fusion power plant conceptual design based on a low aspect ratio 'spherical torus' (ST) plasma. The power core uses an advanced 'dual-cooled' breeding blanket with flowing PbLi breeder and He-cooled ferritic steel structures. The main features of the blanket design are summarized here together with analysis of the thermal hydraulic and thermomechanical performance.

Keywords: Breeding blanket; Fusion; ARIES-ST

1. Introduction

ARIES-ST blanket design choices were influenced strongly by several unique features of the low aspect ratio spherical torus, including: (1) the use of water coolant in the power core (for the copper centerpost) strongly discourages the use of reactive materials such as lithium and beryllium; (2) high thermal conversion efficiency is desirable to offset the effect of high recirculating power in the normal-conducting TF system; (3) relatively high power density results from the extraordinarily high plasma beta, placing constraints on the first wall for surface heat removal; (4) the absence of space on the inboard side for a breeding blanket places additional constraints on material selection and dimensions; and (5) the highly elongated plasma and continuous outboard TF shell led to a vertical maintenance scheme and toroidally integrated blanket.

The combination of high power density (~ 5 MW m^{-2}) with sufficiently high efficiency in the power conversion system can not be achieved with solid breeder blankets irrespective of the structural material used, because the maximum temperature of all candidate breeder materials would exceed specified limits. Self-cooled lithium blankets with vanadium alloy as structural material allow for both high power density and high temperatures. They were avoided in ARIES-ST for safety reasons because water is used within the power core as the TF magnet system coolant. Safety concerns could be overcome by using the eutectic lead lithium alloy PbLi instead of lithium.

* Corresponding author. Tel.: +1-619-5347897; fax: +1-619-5347716.
E-mail address: tillack@fusion.ucsd.edu (M.S. Tillack).

0920-3796/00/$ - see front matter
PII: S0920-3796(00)00366-5

However, the heat transport properties, as well as the compatibility with ferritic steels and vanadium alloys for this liquid metal are not as good as with pure lithium.

The ARIES-ST blanket borrows features from the European Dual-Coolant DEMO blanket [1], and the PbLi-cooled SiC/SiC blanket 'TAURO' [2]. Several design modifications and performance enhancements were made to ensure compatibility with the ARIES-ST plasma and to allow it to meet the requirements for an attractive commercial power plant. Design changes to the blanket as compared with the EU-DEMO design include extension of the power handling capability of the first wall by using an advanced ODS ferritic steel and by obtaining maximum advantage of bulk heating in the deep blanket, use of thermally and electrically insulating SiC inserts instead of coatings to reduce the MHD pressure drop and also to ensure the steel structure remains within its design temperature limits while allowing a PbLi outlet temperature of 700°C, optimization of the channel dimensions, and manifolding consistent with the temperature and design integration constraints.

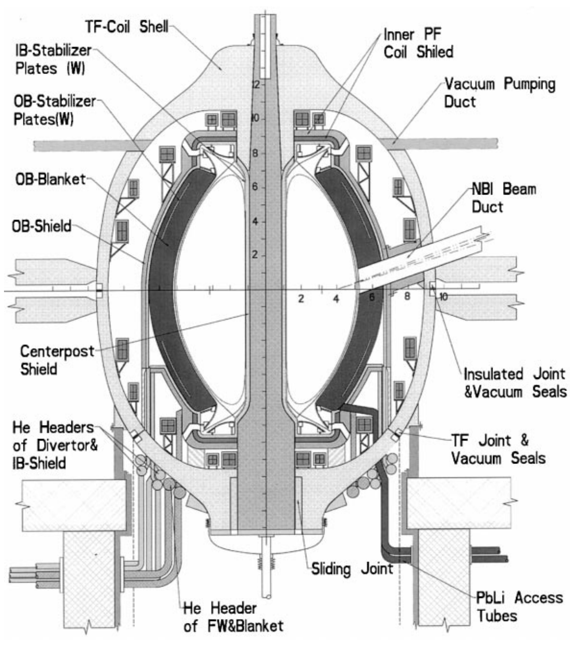

Fig. 1. Elevation view of the ARIES-ST power core.

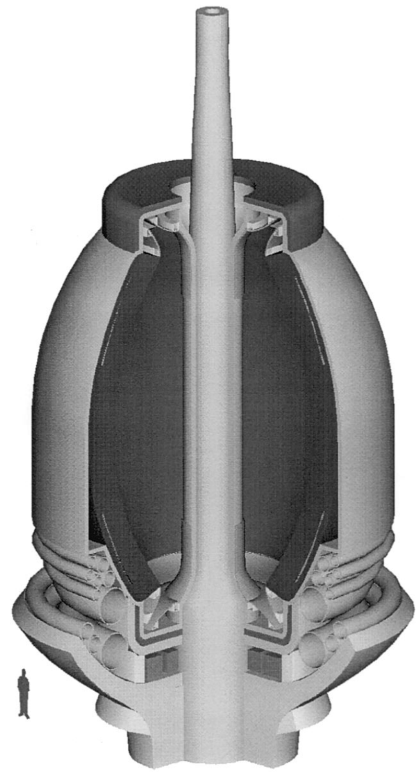

Fig. 2. Power core replacement unit.

2. Power core configuration and power flows

The configuration of ARIES-ST is similar to a 'normal' tokamak with a double null, except that the plasma is highly elongated ($\kappa = 3.75$ at the x-point) to increase the maximum stable plasma beta ($\sim$ 55%). Fig. 1 shows a cross section of the power core in its normal operating position within the vacuum vessel (which also serves as the TF return current leg). Fig. 2 highlights the replaceable power core unit alone, sitting on top of its moveable (reusable) support platform. Single-piece construction is enabled in ARIES-ST by the elongated geometry of the plasma, the ability to provide electrical joints in the normal-conducting TF system, and the relatively small drained weight of a self-cooled blanket ($\sim$ 768 tonnes). Due to the modest replacement cost ($\sim$ \$50 million), efforts to segment the blanket radially and/or re-use parts of the power core were not explored, al-

Table 1
Summary of power flows

Neutron heating	
Total power	
Outboard first wall	100 MW
Blanket steel	330 MW[a,b]
Blanket PbLi	1614 MW[a]
Outboard first wall	
Peak wall load	6.0 MW m^{-2}
Average wall load	4.2 MW m^{-2}
Peak volumetric heating	37 MW m^{-3}
Surface heating	
Outboard first wall	
Peak heat flux	0.6 MW m^{-2}[c]
Average heat flux	0.46 MW m^{-2}
Total power	195 MW

[a] Includes 110 MW conducted from PbLi to He.
[b] Includes heating in manifolds and high-temperature shield.
[c] Design limit is 0.9 MW m^{-2}.

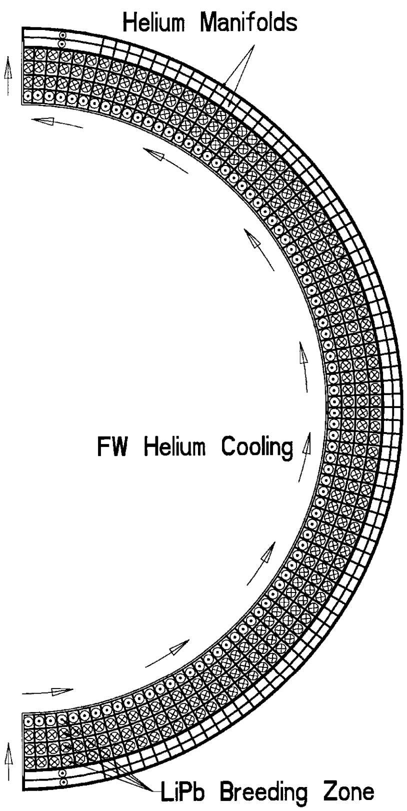

Fig. 3. Mid-plane outboard blanket horizontal cross-section.

though such techniques are possible, and could help reduce the waste stream.

The power core is maintained vertically from below the machine. After the core is drained of the PbLi coolant, the TF joint and vacuum seal can be broken and all coolant lines disconnected in the secondary containment area beneath the core. A system of hydraulic cylinders is used to lower the core onto a rail system and ultimately into an underground vault for hot-cell maintenance. All further maintenance operations are performed in the hot cells after a new replacement core has been installed and power generation has resumed. Further details on the maintenance procedures can be found elsewhere [3].

Plasma edge physics [4] and power core neutronics [5] provided the input power flows used in thermal and mechanical analysis, as summarized in Table 1. Core transport power is partitioned into radiation and particle flows. Since the outboard first wall is positioned well outside the scrape-off layer, the particle flows deposit their energy on the divertor and on the inboard first wall and stability shells. Although the major radius of ARIES-ST is small, the large height results in a first wall area similar to (or larger than) a ‘standard’ aspect ratio tokamak, i.e. 488 m^2. In addition, the plasma volumetric power density is not unusually high. The low toroidal field strength compensates the high average plasma β, such that the volumetric power density — which is proportional to β^2B^4 — is actually smaller than a ‘standard’ aspect ratio tokamak such as ARIES-RS [6]

3. Design description

A cross section of the outboard breeding blanket is shown in Fig. 3. The blanket consists of a helium-cooled ferritic steel first wall with toroidal coolant paths, poloidally-oriented liquid metal ducts defined by internal grid plates, and manifolding.

The first wall box is fabricated by diffusion welding and subsequent bending of the straight plates containing the milled coolant channels [1]. The resulting array of ‘I-beams’ creates stiffness against toroidal bending. This FW forms, to-

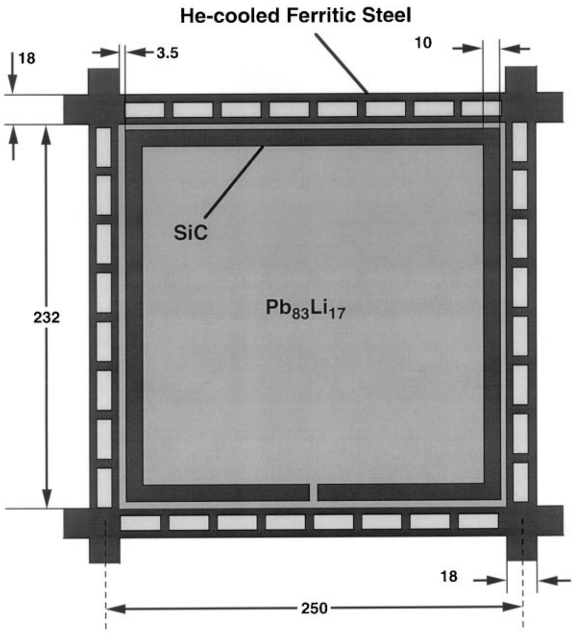

Fig. 4. Cross section of the breeder region unit cell.

gether with the helium manifolds at the back side of the segment, a box containing the flowing liquid metal breeder. One-sided roughening of the coolant channels (on the side nearest the plasma) increases the heat transfer coefficient to the coolant by about a factor of two [7], which lowers the structure peak temperature and temperature variations. Since only one of four walls in a channel is roughened, the increase in pressure drop is modest.

A grid of steel plates inside this box creates large liquid metal ducts and reinforces the FW box, providing stiffness against poloidal bending. They are also fabricated by diffusion welding, similar to the first wall, and are internally cooled by helium. Manifold connections are made in the back of the blanket. Similar to the first wall box, a single vertical weld is performed on each side of the grid plate, rather than attempting to connect each grid plate channel individually. Similar pressures in each subchannel reduces the importance of hermeticity between channels.

Flow channel inserts made of silicon carbide are placed inside the liquid metal ducts (see Fig. 4). These inserts serve as electrical and thermal insulators between the flowing liquid metal and the steel structure. In order to equilibrate pressures and hence reduce stresses on the SiC, an opening is located along the back side and a small gap is provided between the SiC insert and the surrounding walls. A single opening to the electrically conducting structures is expected to have little or no effect on the MHD flow behavior and pressure drop.

The PbLi enters the blanket at the bottom, flows upward in the front row of parallel ducts, turns around at the top by 180° and flows downward in the two parallel rows at the rear of the blanket. In this design, a liquid metal exit temperature of $\sim$700°C is achievable.

The incoming helium at 300°C first cools the first wall in a toroidal configuration between two poloidal manifolds, and then flows poloidally to cool the grid plates, where it is heated up to 525°C. Flowing in series means lower temperatures in the first wall and higher coolant temperatures in regions with lower power density, minimizing temperature differences in the blanket structure. The blanket helium flow is further subdivided into two independent counter-flowing systems. The cooling channels in the first wall as well as those in the grid plates are alternately connected to one of the two systems in order to minimize the temperature increase in case of a loss-of-coolant accident (LOCA) in one of the systems. Another benefit of the alternating flow directions is the more equal temperature distribution in the entire segment, resulting in lower thermal stresses. The temperature of the steel structure is maintained everywhere below 600°C.

High thermal conversion efficiency combined with strong requirements on tritium control and the inherent advantages of an inert gas as working fluid in the cycle led to the choice of a helium Brayton power conversion cycle [8].

To maximize thermal efficiency, the helium exiting the blanket is used as the power cycle working fluid and is heated to its maximum temperature by flowing through an heat exchanger with the high-temperature blanket PbLi as primary fluid. The maximum PbLi temperature of 700°C allows a maximum He temperature to the turbine of 680°C, which enables a net cycle efficiency (including pumping power) of at least

45%. Helium inlet and outlet temperatures are designed to be equal in the blanket, divertor, and inboard first wall and shield. Table 2 summarizes the coolant inlet and outlet temperatures.

The maximum He exit temperature from the blanket is limited by the temperature limitation of the steel to $\sim$525°C. The inlet PbLi temperature of 550°C is selected to provide a temperature difference of 25°C for the design of the PbLi to He heat exchanger. To maximize the He temperature to the turbine with a fixed pinch point temperature, the He inlet temperature to the blanket has to be moderately low. With a He inlet temperature of 300°C, a He temperature of 680°C can be reached. This is the optimum temperature range for the power conversion system.

4. Thermal hydraulic and stress analysis

One of the fundamental requirements on the first wall and blanket is to remain within allowable temperature and stress limits during exposure to normal plasma operation. Ferritic steel is known to be limited in its temperature and stress handling capability by a relatively constrained temperature window and unimpressive thermal conductivity (which leads to high temperatures gradients, increasing both peak temperature and thermal stress). On the low temperature end, concerns over loss of ductility under irradiation suggest a lower limit of 300–350°C [9].

On the high-temperature end, reduced yield strength and thermal creep limit conventional ferritic steel alloys to $\sim$550°C (depending on stress levels and design rules). This upper temperature limit impacts not only the ability to withstand high surface heat flux, but also our ability to operate the gas Brayton cycle with acceptable conversion efficiency. Recent studies suggest that higher-temperature ferritic steels, such as oxide dispersion strengthened (ODS) variants, may be feasible for fusion service conditions [10,11]. If the upper temperature can be increased to 600°C without a commensurate increase in the lower limit DBTT, then an acceptable operating margin is possible for the ARIES-ST first wall design. This maximum temperature occurs only at the outermost surface of the plasma-facing wall and the through-thickness average is below 550°C. Depending on the exact value of stress and the appropriate design rules for the first wall, a peak surface temperature of 600°C may be possible even without the use of more advanced alloys.

For self-cooled blankets, withstanding volumetric heating is not usually a major concern. Peak temperatures and stresses are most severe in the plasma-facing region, where volumetric heating has a significant, but secondary impact. Therefore, the primary focus of thermal–hydraulic analysis was to determine the maximum allowable surface heat flux.

A goal surface heat flux capability of 0.8–0.9 MW m^{-2} on the steel first wall was chosen based on a combination of safety factors and uncertainties. Since previous ferritic steel blanket designs (such as the dual-coolant EU-DEMO design) have not been pushed beyond a surface heat flux of $\sim$0.5 MW m^{-2}, extension of the surface heat flux handling capability was considered important for the success of ARIES-ST.

The thermal–hydraulic heat flux limit is most easily understood in terms of the temperature window of operation. A 'temperature budget' of 300°C exists due to the upper and lower temperature limits of the steel. The bulk temperature rise of 79°C in the first wall is determined by compatibility with the power conversion system, leaving 221°C for conduction and convection. Using one-sided roughening on the plasma-facing wall, the operating window in Fig. 5 is obtained. The upper curve represents the maximum allowable heat flux to maintain the steel within its temperature limit (600°C) whereas the lower curve represents the minimum heat flux required to limit the pumping

Table 2
Power core temperatures

Inlet He temperature	300°C
First wall exit temperature of He	379°C
Blanket exit temperature of He	525°C
Inlet PbLi temperature	550°C
Exit PbLi temperature	700°C
He temperature to the turbine	680°C
Net cycle efficiency	>45%

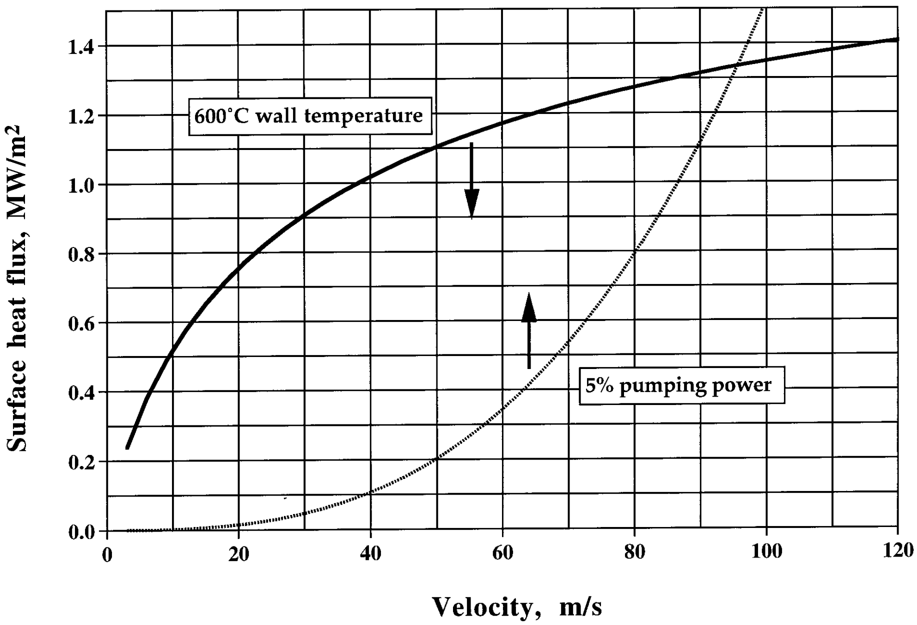

Fig. 5. Heat flux window of operation in the outboard first wall.

Table 3
Von Mises stresses for the first wall at 0.95 MW m^{-2}

Design condition	Temperature (°C)	Calculated peak value (MPa)	Code limit (MPa)
Membrane stress (in web)	500	68	183
Membrane plus bending	580	148	195
Primary plus secondary	575	430	464

power to less than 5% of the thermal power transferred. For these calculations, the channel depth was 25 mm and the first wall thickness was 3 mm.

A 3D stress analysis was performed using the ANSYS code [12] in order to determine the maximum allowable surface heat flux for the reference design (25-mm channel with 3-mm FW). In accordance with the ASME pressure vessel code [13], 'level A' loading allowables were used as follows:

1. Allowable membrane primary stress: 1 S_{mt}
2. Allowable membrane + bending primary stress: 1.5 S_{mt}
3. Allowable primary + secondary stress: 3 S_m

with $S_m = \min(2/3\ \sigma_{0.2}, 1/3\ \sigma_u)$ and $S_{mt} = \min(S_m, 2/3\ \sigma_{R,t}, 1/3\ \sigma_{1,t})$, where $\sigma_{0.2}$ is the 0.2% offset yield stress, σ_u is the tensile strength, $\sigma_{R,t}$ is the creep resistance, $\sigma_{1,t}$ is the 1% creep strain limit, and t is the time to failure, with $t = 2 \times 10^4$ h for end of life. The design allowables for ODS are assumed to have an advantage of 50°C over MANET, so the values for MANET are simply shifted up by 50°C.

Table 3 summarizes the stress analysis results using a uniform surface heat flux of 0.95 MW m^{-2}. The peak primary stress (at the plasma facing wall) is ~ 70 MPa. Note, for the stress analysis, 8 MPa was used for the coolant pressure. The final design point adopted 12 MPa pressure for compatibility with the inboard first wall and divertor plates, such that the stress results must be extrapolated. The primary membrane condition applies in the web where the maximum stress is 68 MPa and the temperature 500°C. This is well below the 1 $S_{m,t}$ limit of 183 MPa for ODS steel and is below the 1 $S_{m,t}$ limit of 165 MPa for MANET. The membrane plus bending condition applies at the first wall where the highest stress is 148 MPa at 580°C. This is well below the 1.5 $S_{m,t}$ limit of 195 MPa for ODS steel, but does not meet the limit of 100 MPa for MANET. Therefore, the proposed design meets the first two criteria for ODS steel, but not MANET.

The highest stress for the combined pressure and thermal loading case occurs in the FW and is 430 MPa at a temperature of 575°C. This is below the 3 S_m limit of 464 MPa for ODS steel but does not meet the 398 MPa limit for MANET. The proposed design meets all of the ASME criteria for ODS steel.

5. Summary

The dual coolant blanket concept has been modified and improved in order to extend its performance characteristics. The addition of SiC flow channel inserts simultaneously eliminates MHD pressure drop as an issue and allows a much higher coolant outlet temperature. The requirements on the SiC insert are so minor that radiation damage and material property degradation are considered insignificant. The major issue arising from the use of SiC and PbLi at high temperature is the development of an acceptable PbLi heat exchanger.

The first wall was modified to withstand higher surface heat flux — as high as 0.9 MW m^{-2}. Further design analysis and testing are needed to confirm this high level of performance in ferritic steel. It is enabled in part by the extended operating temperature window expected with advanced ODS alloys now under development in international fusion programs. One of the consequences of the extended performance capability of the first wall was the inability to withstand an internal coolant rupture in the outer blanket box, which will require demonstration of rupture disks or similar passive safety measures.

References

[1] S. Malang, M.S. Tillack (Eds.), Development of Self-Cooled Liquid Metal Breeder Blankets, FZK-report, FZKA 5581, November 1995.
[2] A.S. Perez Ramirez, A. Caso, L. Giancarli, N. Le Bars, G. Chaumat, J.F. Salavy, J. Szczepanski, TAURO: a ceramic composite structural material self-cooled Pb–17Li breeder blanket concept, J. Nucl. Mater. 233–237 (1996) 1257–1261.
[3] X.R. Wang, M.S. Tillack, F. Najmabadi, S. Malang and the ARIES Team, Configuration and Maintenance of the ARIES-ST Power Plant, Proceedings of the 18th IEEE/NPSS Symposium on Fusion Engineering, Albuquerque, NM, October 1999.
[4] S. Jardin and the ARIES Team, ARIES-ST Physics Analysis, Fus. Eng. Des., to be published.
[5] L. El-Guebaly, I. Sviatoslavsky and the ARIES Team, ARIES-ST Nuclear Analysis and Shield Design, Fus. Eng. Des., to be published.
[6] F. Najmabadi and the Aries Team, Overview of the ARIES-RS Reversed-Shear Tokamak Power Plant Study, Fus. Eng. Des. 39 (1997) 3–25
[7] W.M. Rohsenow, J.P. Hartnett, E.N. Ganic, Handbook of Heat Transfer Applications, second ed., McGraw-Hill, New York, 1985.
[8] S. Malang, H. Schnauder, M.S. Tillack, Combination of a self-cooled liquid metal breeder blanket with a gas turbine power conversion system, Fus. Eng. Des. 39–40 (1998) 561.
[9] M. Rieth, Irradiation Project Manitu 300°C, Review 30 August 1996.
[10] D.K. Mukhopadhyay, F.H. Froes, D.G. Gellis, Development of oxide dispersion strengthened ferritic steels for fusion, J. Nucl. Mater. 258–263 (1998) 1209.
[11] S. Ukai, T. Nishida, T. Okuda, T. Yoshitake, R&D of oxide dispersion strengthened ferritic martensitic steels for FBR, J. Nucl. Mater. 258–263 (1998) 1745.
[12] ANSYS Version 5.3. Swanson Analysis Systems, Houston, PA.
[13] ASME Boiler and Pressure Vessel Code, Section III, Code Case N-47-29, 1995.